 SOLA, 2019, Vol. 15A, 60−65, doi:10.2151/sola.15A-011

Diagnosing Environmental Properties of the July 2018 Heavy Rainfall Event in Japan

Tetsuya Takemi[1] and Takashi Unuma[2]
[1]*Disaster Prevention Research Institute, Kyoto University, Uji, Japan*
[2]*Japan Meteorological Agency, Tokyo, Japan*

Abstract

This study documented the environmental properties of precipitation systems that produced the July 2018 Heavy Rainfall event in Japan. The gridded analysis data were used to diagnose the potential for the development of convective systems in terms of thermodynamic environmental indices. Precipitable water vapor was extremely larger than that seen in the climatology of warm-season quasi-stationary convective clusters (QSCCs). Such an extreme moisture content was realized by very humid conditions at the middle-levels. In contrast, temperature lapse rate in a convectively unstable layer was not so significant in comparison to the QSCC climatology. Among the environmental indices, K Index was shown to describe the potential for the rainfall development. Based on the analysis, the roles of moisture content and profile on the convection development were discussed. It was suggested that the middle-level high humidity contributes to the occurrence of the present heavy rainfall by minimizing negative effects of environmental mixing and by decreasing vertical displacements to reach levels of free convection. In regions where heavy rainfall occurred, an automated algorithm detected the development of QSCCs, which were mostly categorized as a linear type.

(**Citation**: Takemi, T., and T. Unuma, 2019: Diagnosing environmental properties of the July 2018 Heavy Rainfall event in Japan. *SOLA*, **15A**, 60−65, doi:10.2151/sola.15A-011.)

1. Introduction

Heavy rainfalls often occur during the Baiu season in Japan (e.g., Tsuguti and Kato 2014), and some of them spawn floodings, landslides, and other water-related disasters. Recent years faced disaster-spawning extreme events in Japan. In July 2017, heavy rainfall occurred in northern Kyushu, resulting from a long-lasting, linear convective system; the total rainfall exceeded 600 mm in a localized area (Kato et al. 2018; Takemi 2018). While in July 2018, heavy rainfall occurred over widespread areas and caused a large number of fatalities and severe damages (Cabinet Office 2019). The year 2018 was marked not only by this July Heavy Rainfall event but also by the subsequent extreme hot weather (Imada et al. 2019; Nishi and Kusaka 2019) and a number of extreme typhoon landfalls (Takemi et al. 2019).

Extreme weather in summer 2018 was a global phenomenon; heat waves and/or extreme rainfalls almost simultaneously developed in regions of the Northern Hemisphere. Kornhuber et al. (2019) indicated that the extreme events were connected by a hemispheric wavenumber-7 teleconnection pattern. Liu et al. (2019) examined the heat wave in northeast Asia in July 2018 and showed that northward shift of the western North Pacific Subtropical High (NPSH), stimulated by an eastward-propagating wave train originated from Europe, was the cause for the heat wave. The large-scale atmospheric conditions for the extreme rainfall and heat wave in July 2018 in Japan were investigated by Shimpo et al. (2019), who documented that the extreme rainfall was caused by persistent moist airflows and Baiu frontal ascent while the heat wave was due to the enhancement of both surface NPSH and upper-level Tibetan High. In this way, large-scale environmental conditions have been described.

On the other hand, mesoscale aspects of the July 2018 Heavy Rainfall event have not been well documented. Tsuguti et al. (2018) overviewed the rainfall characteristics in July 2018, but did not examined the environmental features. As demonstrated by Chuda and Niino (2005), Nomura and Takemi (2011), and Unuma and Takemi (2016a, hereafter referred to as UT16a; 2016b, referred to as UT16b), diagnosing the environmental properties of convection is useful in order to understand the potential for the development of convective rainfall.

As a preliminary study, we diagnose and document the environmental properties of the July 2018 Heavy Rainfall event in Japan by examining gridded analysis data and compare the properties of the present case with those demonstrated for warm-season, stationary/slow-moving convective systems (called as quasi-stationary convective clusters (QSCCs) in UT16a). A QSCC is defined as a stationary or slow-moving cluster of convective clouds including mesoscale convective systems, rainbands, and other types of convective systems, and is typically a meso-β-scale phenomenon with its shape being mostly linearly elongated (UT16a, UT16b). The development of QSCCs observed in this event is further investigated in light of the environmental analyses.

2. Data and analysis procedure

Three-hourly analysis data from the Mesoscale Model (MSM) of Japan Meteorological Agency (JMA) (Saito et al. 2006) were used to describe the environmental properties in July 2018. By focusing on the initial values of the MSM forecasts, we assess the temporal averaged fields during the heavy rainfall event as the background environment surrounding the rainfall event. In UT16a the convective environments were defined as the conditions *before* the development of convection. However, in the present heavy rainfall event convection successively developed and was widely distributed over the Japanese islands, and thus the *pre-storm* environments are not easily defined in a straightforward way. Therefore, this study examines the environmental conditions as the temporal-averaged fields.

Thermodynamic indices and parameters used for diagnosing environmental conditions favorable for the convective development were examined, as in Bluestein and Jain (1985), Chuda and Niino (2005), Nomura and Takemi (2011), Takemi (2014), and UT16a. The parameters chosen here are convective available potential energy (CAPE), convective inhibition (CIN), precipitable water vapor (PW), K Index (KI) (George 1960), and temperature lapse rate between the levels of 850 hPa and 500 hPa (corresponding well to convectively unstable layer) (TLR; Takemi 2007a, 2007b, 2010, UT16a), as computed from the MSM data. For the readers' convenience, the equation of KI is given here:

$$KI = T_{850} - T_{500} + Td_{850} - (T_{700} - Td_{700}),$$

where T_{850}, T_{700}, and T_{500} refer to temperature at 850, 700, and 500 hPa, respectively, and Td_{850} and Td_{700} denote dew-point temperature at 850 and 700 hPa, respectively. CAPE was computed by adiabatically raising a parcel whose properties are vertically averaged in the lowest layer below the 950-hPa level, similar to UT16a. In addition to these thermodynamic variables, we examined bulk Richardson number (BRN), as in UT16a, to infer the shape of the extracted QSCCs.

We used the rainfall intensity data from the network of the

Corresponding author: Tetsuya Takemi, Disaster Prevention Research Institute, Kyoto University, Gokasho, Uji, Kyoto 611-0011, Japan. E-mail: takemi@storm.dpri.kyoto-u.ac.jp.

operational weather radars of JMA to extract QSCCs. The data have a 1-km resolution with 10-minute interval; the details of the data are described in UT16a. The UT16a algorithm was applied to the radar data by setting the UT16a's definition for QSCCs: the contiguous area of precipitation intensity being equal to or larger than 10 mm h^{-1} is at least 200 km^2; at least one grid overlaps between the two time steps; the maximum motion speed is 10 m s^{-1}; the lifetime is resolved at least three time steps.

All the times herein are referred to as in Japan Standard Time (JST), 9 hours plus UTC.

3. Results

3.1 Environmental conditions

The rainfall distributions in early July of 2018 are demonstrated in Fig. 1. The rainfall amounts were computed by accumulating the Radar-estimated precipitation amount at the 10-minute interval. The period is divided into periods of 3−5 July and 5−8 July. Because of the passage of Typhoon Prapiroon, significant amounts of rainfall during 3−5 July occurred on the Pacific coastal regions in southern Japan. After 5 July, the regions of significant rainfall amounts extended in western and central Japan. In the followings, the period of 5−8 July is focused to document the environmental properties.

The environmental parameters were temporally averaged for the period of 5−8 July and are shown in Fig. 2. CAPE values

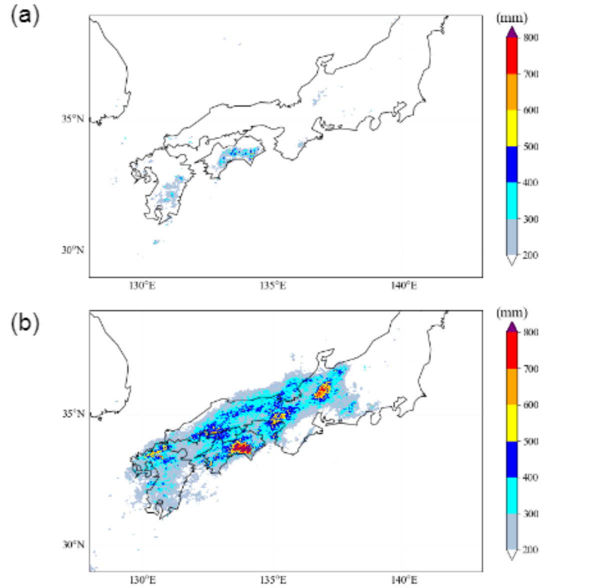

Fig. 1. The accumulated rainfall amount during the period (a) from 0000 JST 3 July to 2350 JST 4 July 2018 and (b) from 0000 JST 5 July to 2350 JST 7 July 2018.

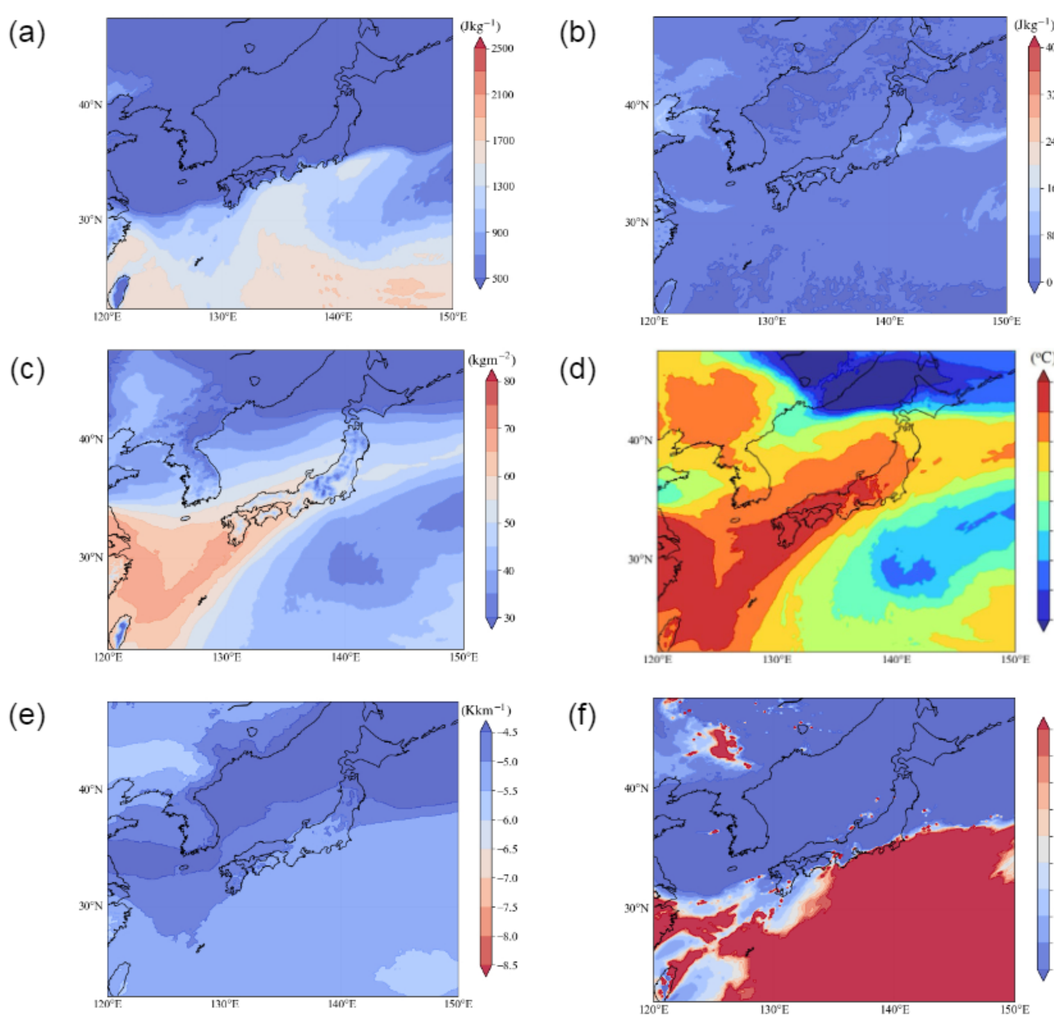

Fig. 2. The temporal mean fields of (a) CAPE (J kg^{-1}), (b) CIN (J kg^{-1}), (c) PW (kg m^{-2}), (d) K Index (°C), (e) TLR (K km^{-1}), and (f) BRN averaged during the period from 0000 JST 5 July to 0000 JST 8 July 2018.

become larger with the southern latitude, as in the climatology shown by Chuda and Niino (2005). Meanwhile, the CAPE values over Japan are not significantly large and comparable to those for the QSCC case in UT16a. CIN is also comparable to the QSCC climatology. In this sense, CAPE and CIN are not so significant for the present event.

In contrast, from East China Sea to western Japan extend areas of high PW exceeding 65 kg m^{-2}, which is well in the higher range of the QSCC climatological values. For example, the 75-percentile values of PW at Fukuoka and Kagoshima in July are 58 and 59, respectively (UT16a). KI exceeds 35, which is also much higher than the July means at Fukuoka, Kagoshima, and other sites in Japan. The high-KI areas also extend from East China Sea toward the Japanese islands, but a distinguishing feature from that of PW is that the high KI area covers western and central Japan, corresponding well with the heavy rainfall region (Fig. 1b). Since PW is a quantity vertically integrated from the surface, the value is generally lower at an elevated location. On the other hand, KI is determined from temperatures and dew-points at 850, 700, and 500 hPa, and hence is not so affected by the ground elevation. This is a reason why the areas of high KI, rather than high PW, correspond well with the heavy rainfall region.

Because KI is partly determined with the temperature lapse rate in the 850−500 hPa layer, TLR is further examined. In Fig. 2e, the absolute value of TLR is seen to vary around 5.5, a little higher than, but almost comparable to the QSCC climatology. Therefore, the contribution to higher KI is mainly from higher dew-points at 850 and 700 hPa.

BRN is less than 10 over the land regions of Japan while is 10−40 off the coasts of Kyushu and Shikoku (Fig. 2f). BRN is generally quite large over the ocean to the south of Japan, because of larger CAPE (Fig. 2a) and low-shear environment under NPSH.

From Fig. 2, PW and KI are found to characterize the significance of the environmental properties for the present heavy rainfall event. Based on this, the PW and KI maxima during the period of 0000 JST 5 and 0000 JST 8 July are further examined. Figure 3 exhibits the spatial distributions of the PW and KI maxima, indicating that the PW maxima are well over 70 and the KI maxima exceed 40 in some locations. Those values are exceptionally larger than the values for QSCC (UT16a).

From these analyses, the large amount of moisture characterizes the condition of the present heavy rainfalls. UT16a indicated that higher amounts of PW for the QSCC environments are due to higher amounts of moisture in the middle layer above the 700-hPa height. As in tropical convection in which higher moisture content is favorable for deeper clouds (Takemi et al. 2004; Derbyshire et al. 2004; Kikuchi and Takayabu 2004; Takemi 2015), UT16a emphasized that higher moisture at middle-levels (i.e., the 3−5 km layer in UT16a) is favorable for the QSCC development. Thus, middle-level relative humidity (RH) fields are demonstrated here.

Figure 4a shows the mean RH averaged vertically in the 700−300 hPa layer and during the period from 0000 JST 5 July to 0000 JST 8 July 2018. A band of higher RH exceeding 80% covers the most part of western and central Japan, corresponding well with the region of high KI (Fig. 2d). The middle-level RH is also greater than the QSCC means at Kagoshima where RH is well below 80% above the 600-hPa level (UT16a). Thus, the mean RH of 80% or higher represents an extremely moist condition. Such a moist middle layer indicates a contrasting feature from that seen before 0000 JST 5 July. Figure 4b indicates that the middle-level RH is drier during 3−5 July than during 5−8 July.

The temporal variation of the middle-level RH is shown in terms of the time and latitude diagram (Fig. 5). The extremely moist middle layer during 5−8 July is seen to be resulted from the merger of middle-level moist regions from the north and the south as seen in the period from 0000 JST to 1200 JST 5 July; after this period the condition of higher RH becomes stationary in the latitudinal region of 32° and 36°N. The radar/raingauge analyzed rainfall (Nagata 2011) is overlaid in Fig. 5. After the merger of the two moist regions, higher rainfall intensities are seen after the time when the middle-level RH exceeds 90%.

The contribution of a layer moisture content to PW in the

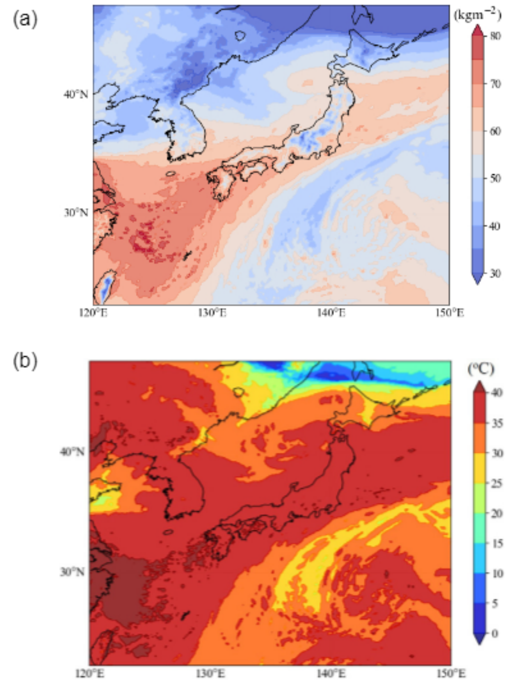

Fig. 3. The spatial distributions of the maximum values of (a) PW and (b) K Index during the period from 0000 JST 5 July to 0000 JST 8 July 2018.

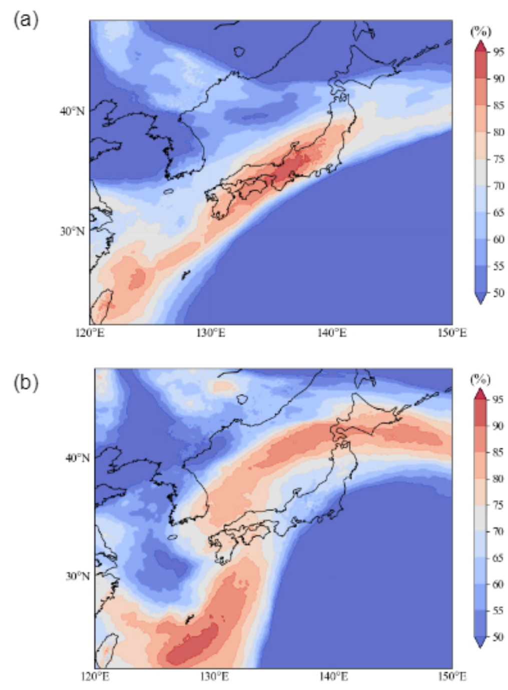

Fig. 4. The temporal mean fields of middle-level relative humidity (vertically averaged in the 700−300 hPa layer) averaged during the period (a) from 0000 JST 5 July to 0000 JST 8 July and (b) from 0000 JST 3 July to 0000 JST 5 July 2018.

130°E−132.5°E longitude is shown in Fig. 6. In the lower layers of 1000−900, 900−800 and 800−700 hPa, the contributions before the noon of 5 July are around 25, 20, and 18%, respectively, which are slightly lower than or equal to the modes for the QSCC environments found in UT16a. In contrast, the contributions for the middle layers of 700−600 and 600−500 hPa are respectively

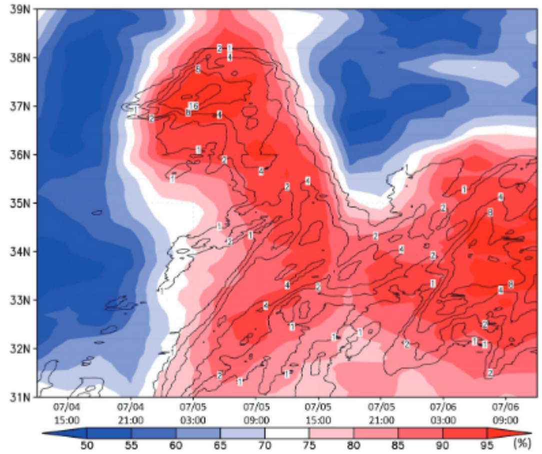

Fig. 5. The time and latitude section of middle-level relative humidity (%, color shading) (vertically averaged in the 700−300 hPa layer and horizontally averaged in the 130°E−132.5°E longitude) as well as the analysis hourly rainfall (mm, contoured) zonally averaged in the 130°E−132.5°E longitude. The rainfall is contoured at the values of 1, 2, 4, 8, and 16. Note that the analysis rainfall is the hourly accumulated value.

around 15 and 10%, higher than the modes for the QSCC cases. Although the moisture content itself is larger at the low-levels than at the middle-levels, the relative contribution of middle-level moisture is high, compared to the QSCC climatology.

We have also examined the contributions of layer moisture contents to PW in different longitudinal bands of 132.5°E−135°E and 135°E−137.5°E (see Fig. 1 for these regions) and found features similar to those shown in Fig. 6. Therefore, the high contributions of middle-level moisture during the present rainfall event are commonly seen in the western part of Japan.

3.2 Quasi-stationary convective clusters

First, we applied the UT16a algorithm to the radar data for the period from 0000 JST 3 July to 0000 JST 5 July and found that the number of detected QSCCs was only 2. This suggests that the environmental condition during this period is not favorable for their developments.

We then extracted QSCCs during the period from 0000 JST 5 July to 0000 JST 8 July and found that the extracted number was 25. The spatial distribution of the QSCC occurrence is demonstrated in Fig. 7. QSCCs distribute in western and central Japan, in accordance with the region of the heavy rainfall. Note that the propagating speeds of ninety-three percent of the extracted QSCCs exceed the mean value of 5.6 m s^{-1} found in UT16a. This seems to

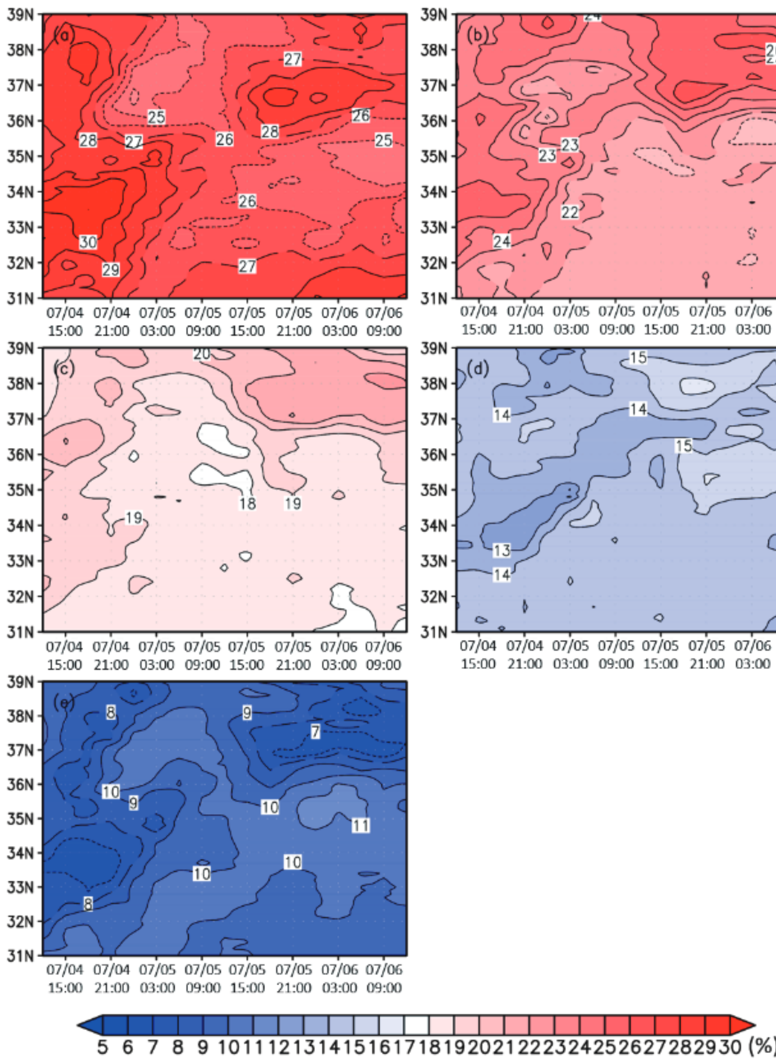

Fig. 6. The time and latitude section of the total water vapor content over layers of (a) 1000−900 hPa, (b) 900−800 hPa, (c) 800−700 hPa, (d) 700−600 hPa, and (e) 600−500 hPa relative (%) to precipitable water vapor. As in Fig. 5, the values are zonally averaged in the 130°E−132.5°E longitude. Solid, dashed, and dotted contour lines indicate the values of the layer-total vapor contents relative to precipitable water being, respectively, larger than, equal to, and smaller than the modes of the QSCC environments in UT16a.

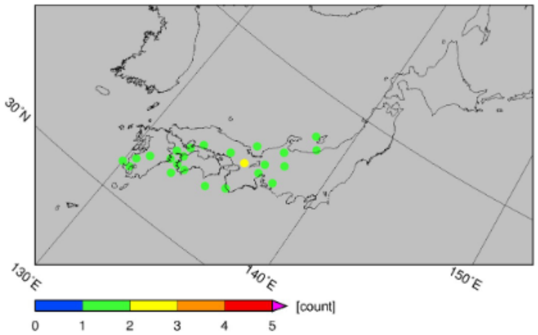

Fig. 7. The spatial distribution of the extracted QSCCs during the period from 0000 JST 5 July to 0000 JST 8 July 2018. The number of the occurrence is indicated in a 50 km by 50 km area, as in UT16a.

be consistent with generally low BRN environments (as compared to UT16b), because strong shears may provide background flows to make QSCCs move faster even when the maximum motion speed is limited to 10 m s^{-1}.

The difference in the number of the QSCCs between the periods before and after 0000 JST 5 July implies that the environmental condition, especially larger PW with moister middle-levels, during 5−8 July is more favorable for the QSCC development than that of 3−5 July. We also examined the shape of the extracted QSCCs by using the UT16b algorithm which fits the QSCC shape to an ellipse and found that the algorithm successfully determined the QSCC shape for 19 cases out of 25 during the period of 5−8 July. Among the 19 QSCCs, 18 cases were shown to have a linear shape (which is defined as having the major-minor-axis ratio of the fitted ellipse equal to or greater than 1.4). This result is consistent with the finding of UT16b. Lower BRN environments are suggested to provide favorable conditions for linear QSCCs.

4. Discussion

The present environmental analysis indicated that a higher amount of moisture along with a humid condition in the middle layer are closely related to the present heavy rainfall event. According to Sekizawa et al. (2019), such an extremely moist condition was generated by enhanced moisture flux from the south toward the Japanese islands, induced by anomalous oceanic evaporation due to intensified low-level winds from the surface to the 925-hPa level and positive anomaly of sea surface temperature, and the enhanced moisture convergence in western Japan. Shimpo et al. (2019) indicated that low- and middle-level southwesterlies from enhanced convection in the southern East China Sea and low-level southerlies from NPSH jointly bring the extreme amount of moisture to Japan. These larger-scale circulation features generate the moist environment favorable for the heavy-rain-producing convective systems. The present analysis clearly demonstrates that the extremely moist condition characterizes the potentially unstable environment for convective outbreak.

Possible reasons why the very humid condition is favorable for convective development are discussed here. One reason is because a moist environment minimizes negative effects of mixing with drier airs outside clouds, as in tropical convection. As indicated in Takemi (2006) and Takemi (2007a), moister environments promote stronger convection than drier environments, if the temperature lapse rate is unchanged. In the present heavy rainfall event, the temperature lapse rate is mostly similar to the QSCC climatology, and hence a tropospheric moisture profile plays a role. Another reason is that the vertical displacements required for boundary-layer air parcels to reach their lifting condensation levels (LCL) and levels of free convection (LFC) are very small, and therefore small amounts of trigger would be sufficient to kick off convection. The idea that smaller vertical displacements to reach LCL/LFC are favorable for convective development was emphasized by Takemi and Satomura (2000) in their squall-line development theory in drier environments. This theory will explain the development and maintenance mechanisms for the present rainfall event. This should be further investigated by numerical experiments.

The analysis on the occurrence of QSCCs indicated that the extracted QSCCs during the present heavy rainfall event have faster propagation speeds than those identified by UT16a. As indicated in UT16a, QSCCs in a faster-moving category have larger precipitation area than those in a slower-moving category. Therefore, such QSCCs are considered to be potentially hazardous through producing widespread rainfall.

5. Conclusions

This study documented the environmental properties for the occurrence of convective systems that produced the extreme rainfall of July 2018 in Japan. The analysis of the environmental parameters typically used to diagnose the potential for the convective development indicated that PW is significantly larger than that found for the QSCC environment. An extremely humid condition at the middle-levels was identified as a characteristic feature for the high PW condition. Among the environmental parameters examined, higher KI was found to correspond well with the region of the heavy rainfall. Because the temperature lapse rate in a convectively unstable layer was not significant, the high RH condition at the middle-levels led to the higher value of KI.

Although KI was one of the classic indices, the utility of KI seems not to be well recognized in studies of convective systems. Takemi (2007a), Nomura and Takemi (2011), Takemi (2014), and UT16a indicated the usefulness of this index to diagnose the mesoscale environment for the development of convective systems. The index can also be used to describe the potential for thunderstorm development under global warming (Takemi et al. 2012; Takemi 2012). The present analysis demonstrated that KI is useful in diagnosing the occurrence of the present heavy rainfall event. Practically, a combination of KI with other indices related to wind speed and/or vertical wind shear may help to increase the validity to diagnose the potential condition for the convective development.

There were 25 occurrences of QSCCs during the period from 0000 JST 5 July to 0000 JST 8 July, in accordance with the locations of the strong rainfall. Most of them have a linear shape and move relatively fast compared to the QSCC standard, probably owing to the lower BRN environments.

Possible roles of the humid condition in developing convection were considered to be firstly to minimize unfavorable effects of mixing with the surroundings and secondly to decrease the vertical displacements required for boundary-layer air to reach LCL/LFC. This point should be numerically investigated in future studies.

Acknowledgments

The comments by the reviewers as well as the editor are greatly acknowledged to improve the original manuscript. We thank Mr. Kentaro Hase for his help in processing the MSM data. The MSM data were obtained from the database of Research Institute for Sustainable Humanosphere, Kyoto University. This work was supported by the MEXT TOUGOU program and JSPS Kakenhi 16H01846 and 18H01680.

Edited by: S. Shimizu

References

Bluestein, H. B., and M. H. Jain, 1985: The formation of mesoscale lines of precipitation: Severe squall lines in Oklahoma during the spring. *J. Atmos. Sci.*, **42**, 1711−1732.

Cabinet Office, 2019: A report on damages by the July 2018 Heavy Rainfall. The version of 1 January 2019 (Available online at http://www.bousai.go.jp/updates/h30typhoon7/pdf/310109_1700_h30typhoon7_01.pdf, accessed 27 May 2019).

Chuda, T., and H. Niino, 2005: Climatology of environmental parameters for mesoscale convections in Japan. *J. Meteor. Soc. Japan*, **83**, 391−408.

Derbyshire, S. H., I. Beau, P. Bechtold, J. Y. Grandpeix, J. M. Piriou, J. L. Redelsperger, and P. M. M. Soares, 2004: Sensitivity of moist convection to environmental humidity. *Quart. J. Roy. Meteor. Soc.*, **130**, 3055−3079, doi: 10.1256/qj.03.130.

George, J. J., 1960: *Weather Forecasting for Aeronautics*. Academic Press, New York, 673 pp.

Imada, Y., M. Watanabe, H. Kawase, H. Shiogama, and M. Arai, 2019: The July 2018 high temperature event in Japan could not have happened without human-induced global warming. *SOLA*, **15A**, 8−12, doi:10.2151/sola.15A-002.

Kato, R., K. Shimose, and S. Shimizu, 2018: Predictability of precipitation caused by linear precipitation systems during the July 2017 Northern Kyushu Heavy Rainfall Event using a cloud-resolving numerical weather prediction model. *J. Disas. Res.*, **13**, 846−859, doi:10.20965/jdr.2018.p0846.

Kikuchi, K., and Y. N. Takayabu, 2004: The development of organized convection associated with the MJO during TOGA–COARE IOP: Trimodal characteristics. *Geophys. Res. Lett.*, **31**, L10101, doi:10.1029/2004GL019601.

Kornhuber, K., S. Osprey, D. Coumou, S. Petri, V. Petoukhov, S. Rahmstorf, and L. Gray, 2019: Extreme weather events in early summer 2018 connected by a recurrent hemispheric wave-7 pattern. *Environ. Res. Lett.*, **14**, 054002, doi:10.1088/1748-9326/ab13bf.

Liu, B., C. Zhu, J. Su, S. Ma, and K. Xu, 2019: Record-breaking northward shift of the western North Pacific Subtropical High in July 2018. *J. Meteor. Soc. Japan*, **97**, 913−925, doi: 10.2151/jmsj.2019-047.

Nagata, K., 2011: Quantitative precipitation estimation and quantitative precipitation forecasting by the Japan Meteorological Agency. *RSMC Tokyo–Typhoon Center Technical Review*, **13**, 37−50 (Available online at http://www.jma.go.jp/jma/jma-eng/jma-center/rsmc-hp-pub-eg/techrev/text13-2.pdf, accessed 3 July 2019).

Nishi, A., and H. Kusaka, 2019: Effect of foehn wind on record-breaking high temperature event (41.1°C) at Kumagaya on 23 July 2018. *SOLA*, **15**, 17−21, doi:10.2151/sola.2019-004.

Nomura, S., and T. Takemi, 2011: Environmental stability for afternoon rain events in the Kanto plain in summer. *SOLA*, **7**, 9−12, doi:10.2151/sola.2011-003.

Saito, K., and co-authors, 2006: The operational JMA nonhydrostatic mesoscale model. *Mon. Wea. Rev.*, **134**, 1266−1298.

Sekizawa, S., T. Miyasaka, H. Nakamura, A. Shimpo, K. Takemura, and S. Maeda, 2019: Anomalous moisture transport and oceanic evaporation during a torrential rainfall event over western Japan in early July 2018. *SOLA*, **15A**, 25−30, doi:10.2151/sola.15A-005.

Shimpo, A., and co-authors, 2019: Primary factors behind the Heavy Rain Event of July 2018 and the subsequent heat wave in Japan. *SOLA*, **15A**, 13−18, doi:10.2151/sola.15A-003.

Takemi, T., 2006: Impacts of moisture profile on the evolution and organization of midlatitude squall lines under various shear conditions. *Atmos. Res.*, **82**, 37−54, doi:10.1016/j.atmosres.2005.01.007.

Takemi, T., 2007a: A sensitivity of squall line intensity to environmental static stability under various shear and moisture conditions. *Atmos. Res.*, **84**, 374−389, doi:10.1016/j.atmosres.2006.10.001.

Takemi, T., 2007b: Environmental stability control of the intensity of squall lines under low-level shear conditions. *J. Geophys. Res.*, **112**, D24110, doi:10.1029/2007JD008793.

Takemi, T., 2010: Dependence of the precipitation intensity in mesoscale convective systems to temperature lapse rate. *Atmos. Res.*, **96**, 273−285, doi:10.1016/j.atmosres.2009.09.002.

Takemi, T., 2012: Projected regional-scale changes in atmospheric stability condition for the development of summertime convective precipitation in the Tokyo metropolitan area under global warming. *Hydrol. Res. Lett.*, **6**, 17−22, doi:10.3178/HRL.6.17.

Takemi, T., 2014: Characteristics of summertime afternoon rainfall and its environmental conditions in and around the Nobi Plain. *SOLA*, **10**, 158−162, doi:10.2151/sola.2014-033.

Takemi, T., 2015: Relationship between cumulus activity and environmental moisture during the CINDY2011/DYNAMO field experiment as revealed from convection-resolving simulations. *J. Meteor. Soc. Japan*, **93A**, 41−58, doi:10.2151/jmsj.2015-035.

Takemi, T., 2018: Importance of terrain representation in simulating a stationary convective system for the July 2017 Northern Kyushu Heavy Rainfall case. *SOLA*, **14**, 153−158, doi:10.2151/sola.2018-027.

Takemi, T., and T. Satomura, 2000: Numerical experiments on the mechanisms for the development and maintenance of long-lived squall lines in dry environments. *J. Atmos. Sci.*, **57**, 1718−1740.

Takemi, T., O. Hirayama, and C. Liu, 2004: Factors responsible for the vertical development of tropical oceanic cumulus convection. *Geophys. Res. Lett.*, **31**, L11109, doi:10.1029/2004GL020225.

Takemi, T., S. Nomura, Y. Oku, and H. Ishikawa, 2012: A regional-scale evaluation of changes in environmental stability for summertime afternoon precipitation under global warming from super-high-resolution GCM simulations: A study for the case in the Kanto Plain. *J. Meteor. Soc. Japan*, **90A**, 189−212, doi:10.2151/jmsj.2012-A10.

Takemi, T., T. Yoshida, S. Yamasaki, and K. Hase, 2019: Quantitative estimation of strong winds in an urban district during Typhoon Jebi (2018) by merging mesoscale meteorological and large-eddy simulations. *SOLA*, **15**, 22−27, doi:10.2151/sola.2019-005.

Tsuguti, H., and T. Kato, 2014: Objective extraction of heavy rainfall events and statistical analysis on their characteristic features. *Tenki*, **61**, 455−469 (in Japanese).

Tsuguti, H., N. Seino, H. Kawase, Y. Imada, T. Nakaegawa, and I. Takayabu, 2018: Meteorological overview and mesoscale characteristics of the Heavy Rain Event of July 2018 in Japan. *Landslides*, **16**, 363−371, doi:10.1007/s10346-018-1098-6.

Unuma, T., and T. Takemi, 2016a: Characteristics and environmental conditions of quasi-stationary convective clusters during the warm season in Japan. *Quart. J. Roy. Meteor. Soc.*, **142**, 1232−1249, doi:10.1002/qj.2726.

Unuma, T., and T. Takemi, 2016b: A role of environmental shear on the organization mode of quasi-stationary convective clusters during the warm season in Japan. *SOLA*, **12**, 111−115, doi:10.2151/sola.2016-025.

Manuscript received 31 May 2019, accepted 11 August 2019
SOLA: https://www.jstage.jst.go.jp/browse/sola/